ASM Sc. J., 11, Special Issue 2, 2018 for SANREM, 36-48

Debris Flow Susceptibility Assessment at A Basin Scale: A Case Study at Bundu Tuhan, Ranau, Sabah, Malaysia

Edgar Jr. Joe[1,2*], Felix Tongkul[2,3] and Rodeano Roslee[2,3]

[1]*Slope Branch, Public Works Department of Sabah, Jalan Sembulan, 88852 Kota Kinabalu, Sabah, Malaysia*

[2]*Natural Disaster Research Centre (NDRC), University Malaysia Sabah (UMS), Jalan UMS, 88400 Kota Kinabalu, Sabah, Malaysia*

[3]*Faculty of Science and Natural Resources (FSSA), University Malaysia Sabah (UMS), Jalan UMS, 88400 Kota Kinabalu, Sabah, Malaysia*

Debris flow occurrence is quite common in mountainous areas such as those in the Crocker Range of Sabah, Malaysia especially during prolonged heavy rainfall. While the risk posed by debris flow is enormous, study on its susceptibility level is lacking in Sabah. In the absence of a proper study, the mitigation strategy to address the debris flow hazard appears to be carried out on an ad-hoc basis. This study aims to determine the susceptibility level of debris flow at a basin scale which will be useful for mitigation purpose. Based on a case study at Bundu Tuhan, Ranau, the mapping of debris flow susceptibility level by using Frequency Ratio model displays that most of the study basin is covered by low class which constitutes 49.64% of the total study basin area. The debris flow occurrence is predominantly governed by the causative factor of Normalized Difference Vegetation Index followed by the distance to stream and stream density. The validation of the predictive model also shows that the Frequency Ratio method gives a good success rate of 86%, thus it can be used as a reliable tool to reduce the potential hazard associated with debris flow in the study area.

Keywords: Debris flow, susceptibility, basin, Frequency Ratio, Sabah

I. INTRODUCTION

Numbers of debris flow occurrence have been recorded in Sabah, Malaysia which posed high hazard and risk to the public, especially along the major road in the Crocker Range. The incidents have not only caused disruption in traffic flow due to road closure for several hours but also detrimental effect on social and economic aspects of the public. On the other hand, uncontrolled human activity especially slash-and-burn for traditional farming within the watershed in the Crocker Range has become phenomena for years. The poor planning of land use which may lead to debris flow occurrence is due to lack of understanding of the controlling factor. A less appropriate measure has also been taken to control that activity which is likely due to deficient planning. Therefore, this study aims to analyse the susceptibility level of debris flow at a basin scale based on identified conditioning factor. The mapping of debris flow susceptibility at a basin scale will serve as a tool for planning of land use by the decision-maker.

*Corresponding author's e-mail:

II. STUDY AREA

The study area at Bundu Tuhan, Ranau as shown in Figure 1 is lying in the Crocker Range of Sabah. The mountainous terrain of Crocker Range is averagely elevated at 2,000m high above mean sea level (AMSL) and exhibits a width of more than 40 km which extends about 200 km along the west coast of Sabah. It is bounded by the latitude of 6000'40" N to 6001'00" N and longitude of 116030'30" E to 116031'0" E. The total area of the basin is 113.27 ha. About 85 m long and 20 m wide road section is affected due to the debris flow. The study area covers the distance of 0.23 km from north to south and 0.30 km from west to east. The study area is also underlain by undulating mountainous landform which varies from 875 m AMSL to 1,678 m AMSL. It is populated by moderate to dense natural stream lying in the deep valley between adjacent hillsides.

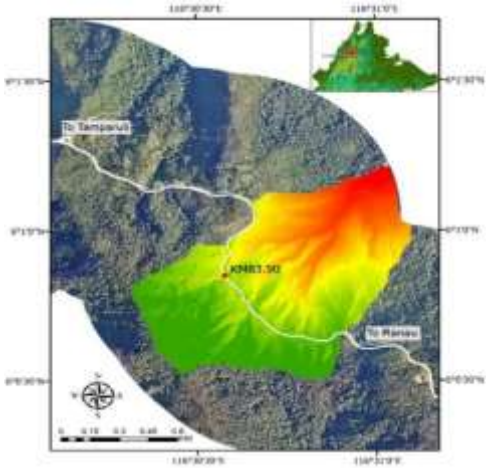

Figure 1. Location of study basin at sub-catchment of Bundu Tuhan area in Ranau.

A well-known debris location at KM 83.90 of Jalan Tamparuli-Ranau is situated within the study basin. Series of debris flow events have been recurring in the year 2012 to 2014 at similar location. The incidents have not only caused disruption in traffic flow due to road closure for several hours, but also detrimental effect to social and economic aspects of the public.

III. MATERIALS AND METHODS

Susceptibility analysis of the debris flow at a basin scale is then carried out using the Frequency Ratio model in GIS environment. The modelling involves three stages namely data preparation, analysis, and validation.

In the data preparation, the debris flow distribution is mapped in an orthophoto. Then, nine thematic maps of the causal factors are prepared which pertain to slope aspect, distance to stream, elevation, gradient, vegetative cover, plan curvature, profile curvature, soil cover thickness, and stream density.

In the analysis stage, the frequency ratio for each causal parameter is calculated by applying Equation 1 (Esper Angillieri, 2013).

$$FR = \frac{N(i)/N}{S(i)/S} \quad (1)$$

where

FR = Frequency ratio

N(i) = Number of pixels in which debris flow occur in i variable

N = Number of pixels with debris flow occurrence

S(i) = Number of pixels of i variable

S = Total number of pixels

Factor class with a frequency ratio value of greater than 1 indicates higher probability landslide occurrence, showing a closer relationship between debris flow and the parameter being studied (Saadatkhah et al., 2015). The predictor rate for every spatial factor is calculated using Equation 2 (Althuwaynee et al., 2014).

$$PR = \frac{FR_{max} - FR_{min}}{(FR_{max} - FR_{min})_{min}} \quad (2)$$

where

PR = Predictor rate

FR = Frequency ratio

Then, debris flow susceptibility index is calculated using Equation 3 by summing the multiplication value of predictor rate and frequency ratio of all raster maps of debris flow causal factor (Jaafari et al., 2014).

$$DFSI = \Sigma(PR \times FR) \quad (3)$$

where

DFSI = Debris flow susceptibility index

PR = Predictor rate

FR = Frequency ratio

A higher value of DFSI indicates higher susceptibility to debris flow while a lower value lower of DFSI shows lower susceptibility to debris flow (Rasyid et al., 2016).

Lastly, in the validation stage, Area Under the Curve (AUC) of the Receiver Operating Characteristic (ROC) is used to check the performance of the model. The AUC success curve was counted based on DFSI map as test variable and debris flow distribution for validation as state variable. In order to classify the success rate curve, the value ranges from 50 to 60 % (fail), 60 to 70 % (poor), 70 to 80 % (fair), 80 to 90 % (good), and 90 to 100 % (excellent). It is also generally assumed that most of the debris flow for validation should fall on high or very high susceptibility category (Rasyid et al., 2016). Upon achievement of acceptable success rate, debris flow susceptibility map is finally produced by reclassifying DFSI map into equal break (Meten et al., 2015).

IV. RESULTS AND DISCUSSIONS

A. Distribution of Debris Flow

Debris flow location within the study basin in Bundu Tuhan, Ranau is mapped as illustrated in Figure 2. As all of the data captured pertain to those that occur along the major roads which have affected human life, poor record of debris flow occurrence is available. Thus, only one location of debris flow has been identified. The debris flow is situated in the upper part of the basin towards the southwest. The area of the debris flow is 0.22 ha which covers about 0.19 % of the basin area.

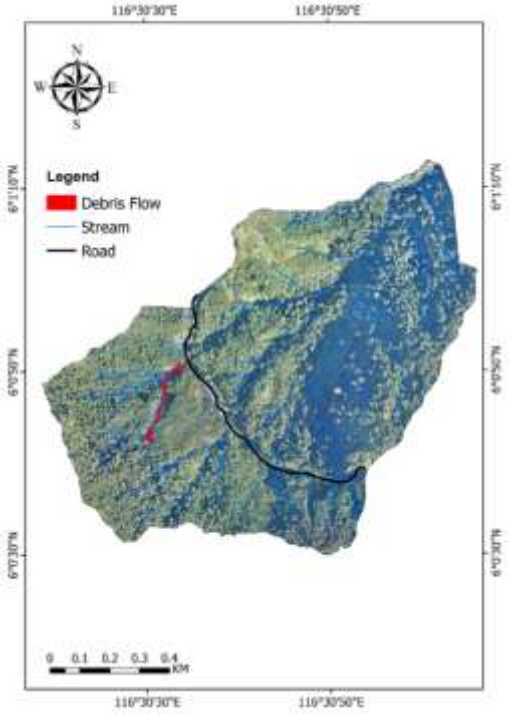

Figure 2. Distribution of debris flow at basin scale in sub-catchment of Bundu Tuhan, Ranau

B. Causal Factor of Debris Flow

Assessment of debris flow susceptibility at a basin scale in Bundu Tuhan, Ranau constitutes the analysis of nine causal factors, which include slope aspect, distance to stream, elevation, gradient, normalized difference vegetation index (NDVI), plan curvature, profile curvature, soil cover, and stream density. Thematic maps, which show the distribution of various classes within each causal factor in the basin, are shown in Figure 3(a) to Figure 3(i).

In terms of slope aspect, the slope orientations are reclassified into eight classes namely north, northeast, east, southeast, south, southwest, west, and northwest (Figure 3(a)). The basin is mostly oriented towards the northeast direction which covers 28.71 % of the total area and mainly occurs towards the south and southwest of the basin. Only 0.21 % of the basin area shows direction towards the southwest which are randomly distributed.

The distances to stream are reclassified into six classes which are 0 m to 20 m, 20 m to 40 m, 40 m to 60 m, 60 m to 80 m, 80 m to 100 m, and exceeding 100 m (Figure 3(b)). About 46.78 % percent of the basin area situated at a distance between 0 m and 20 m to the adjacent stream. The farther areas are situated more than 100 m from the stream which comprise only 0.88 % of the catchment.

The elevation thematic map is comprised of eight classes that pertain to below 1,000 m, 1,000 m to 1,100 m, 1,100 m to 1,200 m, 1,200 m to 1,300 m, 1,300 m to 1,400 m, 1,400 m to 1,500 m, 1,500 m to 1,600 m, and above 1,600 m (Figure 3(c)). Most of the basin areas are elevated at an altitude between 1,200 m and 1,300 m AMSL that comprise 18.63 % of the study basin that occur towards the southwest. The minimum coverage of elevation is 3.31 %, which pertain to a height below 1,000 m AMSL occurring towards the basin northeast.

In Figure 3(d), the five classes of reclassified slope gradient constitute degree from 0 to 20, 20 to 40, 40 to 60, 60 to 80, and more than 80. Majority of the slope gradients fall in class 200 to 400 that covers 62.25 % of the basin area and randomly distributed. The least coverage of slope gradient occurs in class more than 60 degrees, about 0.27 % of the total area which are also scattered in the basin.

The causal factor of NDVI is composed of five classes namely lesser than 0.4, 0.4 to 0.5,

0.5 to 0.6, 0.6 to 0.7, and more than 0.7 (Figure 3(e)). The NDVI value indicates the density of vegetative cover where the higher the value, the dense the vegetation. The highest percentage of NDVI observed is within the range of 0.6 to 0.7, which include 68.54 % of the study are and randomly distributed in the basin. The lowest percentages of NDVI which cover an area of 0.24 % pertain to a class lower than 0.4 and are also scattered within the basin.

The plan curvatures are reclassified into three classes that are the concave, linear, and convex (Figure 3(f)). The concave curvature forms most of the basin with a percentage of 50.38 % that are randomly distributed within the study basin. None of the basin area display linear landform.

Similar to the plan curvature, the profile curvatures are also reclassified into the three classes (Figure 3(g)). The maximum coverage of profile curvature which is 50.45 % occurs in convex curvature and scattered within the study basin. None of the basin area display linear landform.

As shown in Figure 3(h), the soil covers are reclassified into nine classes that are lesser than 5 m, 5 m to 6 m, 6 m to 7 m, 7 m to 8 m, 8 m to 9 m, 9 m to 10 m, 10 m to 11 m, 11 m to 12 m, and more than 12 m. Most of the soil cover belongs to 5 m to 6 m, which comprise 86.25 % of the study basin and are randomly distributed. Only 0.02 % of the area indicates soil cover with a thickness between 9 m and 10 m which are also scattered.

The stream density map is composed of seven classes namely 0 km/km^2 to 10 km/km^2, 10 km/km^2 to 20 km/km2, 20 km/km^2 to 30 km/km^2, 30 km/km^2 to 40 km/km^2, 40 km/km^2 to 50 km/km^2, 50 km/km^2 to 60 km/km^2, and exceeding 60 km/km^2 (Figure 3(i)). Most of the streams exhibit a density of 0 to 10 km/km^2 with a percentage of 37.49 % which mainly occur at the junction of the stream tributaries. The minimum percentage of stream density is 0.04 %, which fall into the category of more than 60 km/km^2 and observed in the area with the absence of stream.

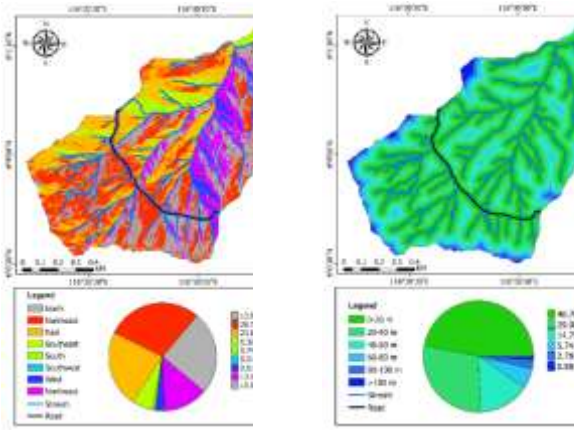

(a) (b)

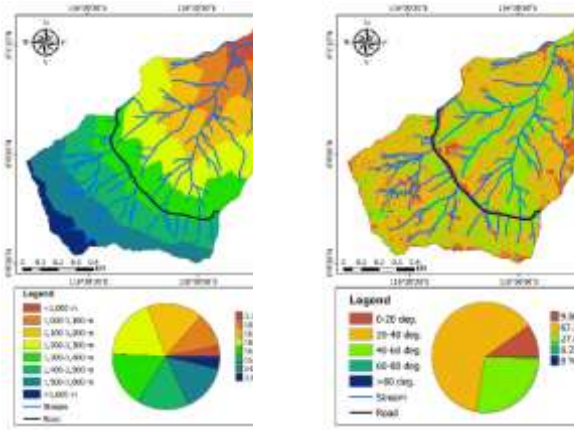

(c) (d)

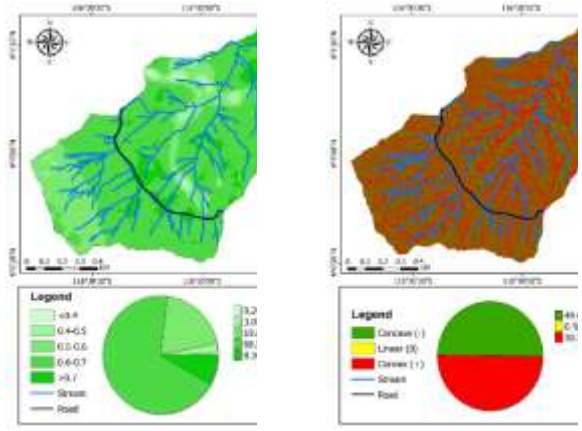

(e) (f)

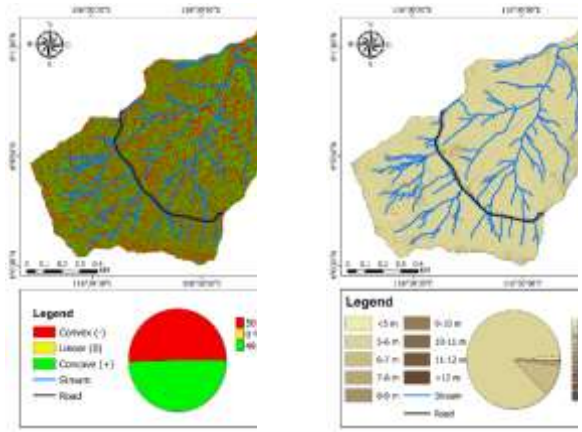

(g) (h)

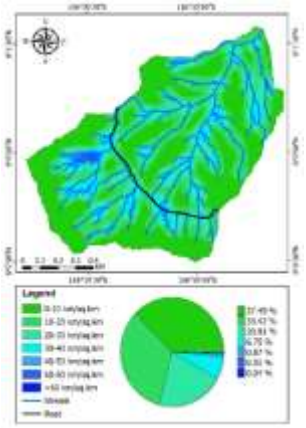

(i)

Figure 3. Thematic map of debris flow causal factors: (a) slope aspect, (b) distance to stream, (c) elevation, (d) gradient, (e) NDVI, (f) plan curvature, (g) profile curvature, (h) soil cover, (i) stream density

C. Frequency Ratio with Conditioning Factor

The computed frequency ratios within each conditioning factor are shown in Figure 4(a) to Figure 4(i).

Variation of computed frequency ratio in slope aspect (Figure 4(a)) shows that majority of the debris flow probability occur on the slope facing towards north direction within the orientation between 00 and 22.50. The maximum frequency ratio is 0.23. It can be anticipated that the area facing in that direction experienced relatively high rainfall which brings higher moisture content, thus prone to debris flow. This corresponds to the findings by other researchers such as Tangestani (2004) and Clerici et al. (2006). On the other hand, lowest probability of debris flow happens on the slope facing west which pertains to a frequency ratio of 0.02. These areas are most likely receiving more sunlight compared to other areas which cause drier ground.

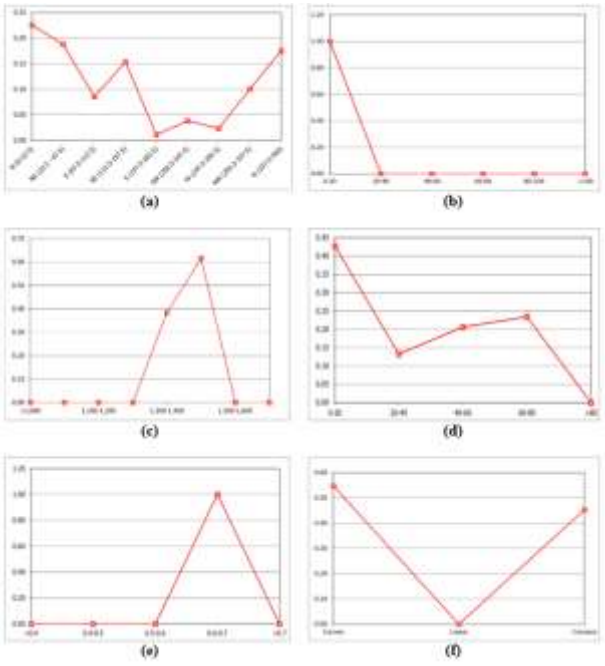

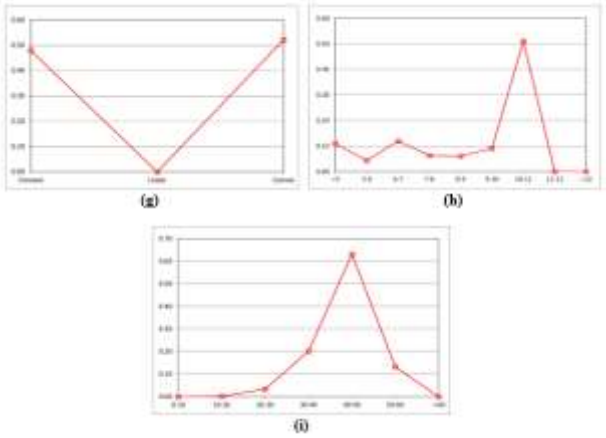

Figure 4. Variation of computed frequency ratio within conditioning factor: (a) slope aspect, (b) distance to stream, (c) elevation, (d) gradient, (e) NDVI, (f) plan curvature, (g) profile curvature, (h) soil cover, (i) stream density

The maximum frequency ratio within the factor of distance to stream is 1.00 which fall in class 0 m to 20 m as shown in Figure 4(b). The class shows a high probability of debris flow as the nearby stream will increase erosion activity at slope toe, thus facilitate the initiation of debris flow. A sharp decrease in debris flow probability is observed with increase in distance to stream as the presence of stream is necessary to mobilise the sediment. This finding is in agreement with the statement by other researchers such as Dai et al. (2001), Jaafari et al. (2014), and Rasyid et al. (2016).

Majority of the debris flow probability distributed within elevation class between 1,400 m and 1,500 m AMSL which exhibit frequency ratio of 0.62 as shown in Figure 4(c). The occurrence of debris flow on this high altitude is associated with low vegetation growth, active soil erosion, higher stream incision, and increasing rainfall intensity. Meanwhile, the elevation below 1,300 m AMSL shows no indication of debris flow probability as low-lying areas are usually covered by thicker soil mantles which require higher groundwater level to initiate the debris flow. Higher altitude of more than 1,500 m AMSL also exhibits zero frequency ratio which most probably is due to a stable slope on higher ground. Other researchers like Dai et al. (2001), Lan et al. (2004), and Tangestani (2004) retain the same convention as proposed in this study findings.

In Figure 4(d), it is found that the maximum frequency ratio within the factor of gradient is 0.43 which pertain to the slope between 00 and 200. The gentler gradient coupled with the presence of stream have favoured water ponding on the slope, thus facilitate debris flow occurrence. Gentler slope is also normally associated with an abundant supply of material as stated by Cevik and Topal (2003). As the gradient increases from 20 to 800, the frequency ratio is also increasing from 0.13 to 0.23. This finding correlate well with the previous study by Dai et al. (2001), Lee and Choi (2004), and Meten et al. (2015) who mentioned that more slope instability occurred on the steeper ground due to increase in shear stress by gravity force. On the contrary, lowest frequency ratio is observed at the gradient of more than 800. This result corresponds with finding proposed Ballantyne (2004) and Rasyid et al. (2016) who mentioned that steep natural slope with outcrop presence exhibits higher strength and less susceptible to shallow landslide due to scarce amount of soil cover.

The NDVI value with the highest frequency ratio of 1.00 falls within the range between 0.60 and 0.70 (Figure 4(e)). In this study, this range considered to be the probable condition for the occurrence of debris flow as the vegetative cover within this class provides insufficient ground canopy for soil protection against erosion. On the other hand, the lowest frequency ratio of NDVI which is 0.00 happen at two separate classes of below 0.60 and above 0.70. For those NDVI class lesser than 0.60, it is anticipated that scarce vegetative cover poses direct exposure of the area to sunlight, thus causing drier ground. Meanwhile, the higher side of NDVI with a value greater than 0.70 shows denser vegetative cover which protects the slope against direct rainwater effect. Other researchers such as Yalcin et al. (2011), Chao et al. (2016), and Sujatha and Sridhar (2017) have identified similar findings.

As stated in previous studies by Reneau and Dietrich (1987), a slope on concave plan curvature is prone to landslide occurrence due to water convergent. However, due to smaller area distribution of convex plan curvature in this study, the convex profile shows the highest probability of debris flow with frequency ratio 0.55 as shown in Figure 4(f). Meanwhile, the lowest frequency ratio happens in linear class due to uniform distribution of surface runoff, posing insignificant effect of slope erosion.

In terms of profile curvature, the maximum frequency ratio is 0.52, in which the highest debris flow probability happens on the convex slope as explained in Figure 4(g). Convex slope shows higher debris flow susceptibility as the slope profile which forms "waterfall" like feature may facilitate surface runoff acceleration. This finding is in agreement with the previous study by Lee and Talib (2005), Nettleton et al. (2005), and Rasyid et al. (2016). On the contrary, the linear profile curvature displays lowest frequency ratio of 0.00 as this profile does not give high effect to the rate of surface runoff movement.

Soil cover with a thickness of less than 5 m to 10 m indicates fluctuating pattern of increase and decrease in frequency ratio ranging from 0.11 to 0.09 (Figure 4(h)). This pattern is most likely governed by other causal factors especially in terms of distance to stream and stream density. Presence of stream with greater force of gushing water is able to mobilize thicker soil cover. This can be observed at thickness 10 m to 11 m which shows maximum frequency ratio of 0.51. As the soil cover increases, the frequency ratio is sharply reduced. Higher water infiltration is required to mobilise loose soil of huge volume. Upon reaching soil thickness of more than 11 m, the frequency ratio shows value of 0.00. Researchers such as Tangestani (2004) and Xiaoqing et al. (2015) also conclude similar result.

Stream density between 40 km/km^2 and 50 km/km^2 displays maximum frequency ratio value equivalents to 0.63 (Figure 4(i)). In this study, the stream density within the class provides sufficient water to mobilize the sediment. On the contrary, researchers like Onda (1993) and Hasegawa et al. (2013) mentioned that landform with higher stream

density should be more susceptible to debris flow as higher drainage density may reduce infiltration rate and increase movement of surface flow.

D. Prediction Rate of Causal Factor

The classification of prediction rate according to their priority is given in Figure 5.

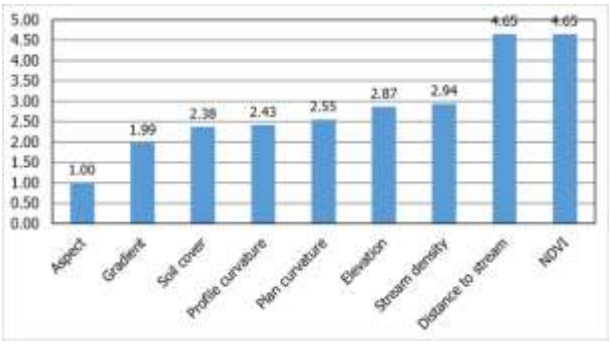

Figure 5. Causal factors of debris flow according to priority

As the causal factors in Figure 5 predominantly display prediction rate value of more than 1.00 (89%), they exhibit a stronger relationship with debris flow probability. This statement is in agreement with that proposed by Saadatkhah et al. (2015). Both the NDVI and distance to stream factors display the highest prediction rate of 4.65 which governs the susceptibility of debris flow at the basin in sub-catchment of Bundu Tuhan, Ranau. The main controlling factors are followed by the stream density with predictor rating of 2.94. On the other hand, the aspect factor shows the minimum effect to the debris flow susceptibility as given by its prediction rate of 1.00.

E. Mapping of Debris Flow Susceptibility

By using the computed prediction rate result for each factor in Figure 5, the Debris Flow Susceptibility Index (DFSI) for this study basin is calculated by applying the proposed following Equation 4.

$$\begin{aligned} DFSI = {} & 1.00\ (\text{aspect}) + 4.65\ (\text{distance to stream}) + \\ & 2.87\ (\text{elevation}) + 1.99\ (\text{gradient}) + 4.65\ (\text{NDVI}) + \\ & 2.55\ (\text{plan curvature}) + 2.43\ (\text{profile curvature}) + \\ & 2.38\ (\text{soil cover}) + 2.94\ (\text{stream density}) \end{aligned} \quad (4)$$

Map of debris flow susceptibility at a basin scale in the study area at Moyog, Penampang is shown in Figure 6. The zones of susceptibility are divided into three classes namely low, medium, high, and very high by equal reclassification of debris flow prone areas.

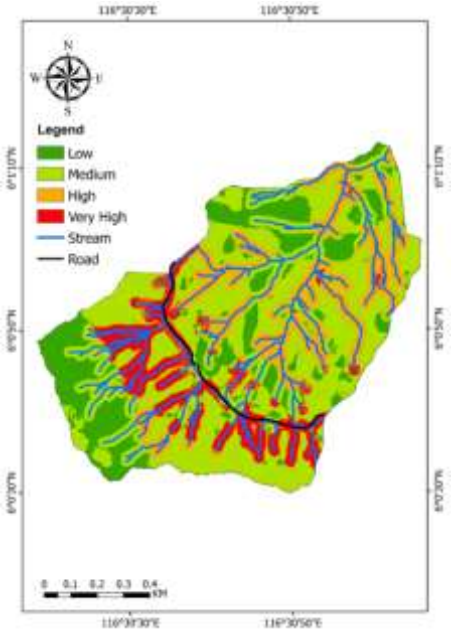

Figure 6. Map of debris flow susceptibility for study area in Bundu Tuhan, Ranau

Characteristic of the susceptibility classes in Figure 7 shows that all of the debris flows occur in a very high zone (0.51 % of the total susceptibility area) which constitute 97.30 % of the total debris flow area. This result corresponds with the finding by Rasyid et al. (2016) who mentioned that the debris flow used for validation should fall into high or very high susceptibility class. On the other hand, no debris flow areas are covered in the area of low and medium susceptibility level. This is due to the limitation in the mapping of debris flow distribution as previously discussed.

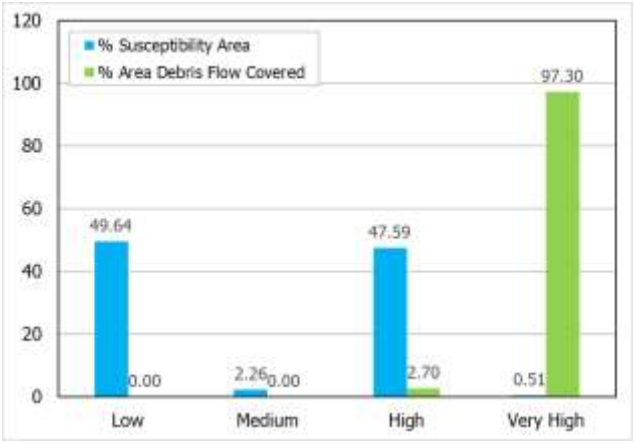

Figure 7. Percentage of susceptibility class and percentage of debris flow on susceptibility map for study area in Bundu Tuhan, Ranau

F. Validation

The success rate curve for the predictive model of debris flow susceptibility analysis for the study area in Bundu Tuhan, Ranau as shown in Figure 8 explains that the test falls in a good category as the 86 % of the area is covered in the curve. A steady increase in the index rank between 0 % and 24 % can explain 100 % of the debris flow.

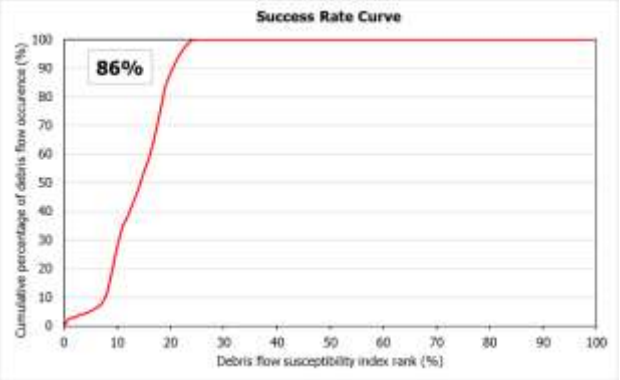

Figure 8. Success rate curve of predictive model of debris flow susceptibility at study area in Bundu Tuhan, Ranau

V. SUMMARY

The debris flow susceptibility mapping at a basin scale in the study area at Bundu Tuhan, Ranau has successfully identified the distribution of susceptibility classes pertaining to low (49.64 %), medium (2.26 %), high (47.59 %), and very high (0.51 %). The contribution of the nine identified causal factors on the debris flow occurrence has also been prioritized, in which the NDVI factor shows the most significant influence followed by the distance to stream and stream density. By modelling the susceptibility class of the study area, local land use planning of the study area can be conducted in order to mitigate future debris flow incident. As given by the acceptable success rate of the predictive model of 86%, the statistical Frequency Ratio method serves as a good tool in mapping debris flow susceptibility in the study area. However, it is recommended that the modelling using statistical methods such as logistic regression and artificial neural network should be tested in order to compare

the performance of each model, as well as to identify the most suitable model which may be applicable to the specific study area. In addition, a comprehensive data collection and record of debris flow occurrence at basin scale should be conducted by interpreting a high-resolution aerial image and verified on site. However, the field work will consume more time and effort especially that which involve vast and remote basin area.

VI. ACKNOWLEDGMENT

The authors would like to thank Public Works Department of Sabah for supplying the data of Digital Elevation Model (DEM) which is very crucial in this study.

[1] Althuwaynee, O. F., Pradhan, B., Park, H. -J., & Lee, J. H. (2014). A novel ensemble bivariate statistical evidential belief function with knowledge-based analytical hierarchy process and multivariate statistical logistic regression for landslide susceptibility mapping. Catena, 114, 21–36.

[2] Ballantyne, C. K . (2004). Geomorphological changes and trends in Scotland: debris-flows. Scottish Natural Heritage Commissioned Report No. 052.

[3] Cevik, E. & Topal, T. (2003). GIS-based landslide susceptibility mapping for a problematic segment of the natural gas pipeline, Hendek (Turkey). Environmental Geology. 44, 49–962.

[4] Chao, M., Yu-jie, W., Cui, D., Yun-qi, W., & Yun-peng, L. (2016). Variation in initiation condition of debris flows in the mountain regions surrounding Beijing. Geomorphology. 273, 323–334.

[5] Clerici, A., Perego, S., Tellini, C. & Vescovi, P. (2006). A GIS-based automated procedure for landslide susceptibility mapping by the Conditional Analysis method: the Baganza valley case study (Italian Northern Apennines). Environmental Geology. 50, 941–961.

[6] Dai, F. C., Lee, C. F., Li, J. & Xu, Z. W. (2001). Assessment of landslide susceptibility on the natural terrain of Lantau Island, Hong Kong. Environmental Geology. 40(3), 381–391.

[7] Esper Angillieri, M. Y. (2013). Debris flow susceptibility mapping in a portion of the Andes and Preandes of San Juan, Argentina using frequency ratio and logistic regression models. Earth Sciences Research Journal. 17(2), 159–167.

[8] Hasegawa, S., Nonomura, A., Nakai, S. & Dahal, R. K. (2013). Drainage density as rainfall induced landslides susceptibility index in small catchment area. International Journal of Landslide and Environment. 1(1), 27–28.

[9] Jaafari, A., Najafi, A., Pourghasemi, H. R., Rezaeian, J. & Sattarian, A. (2014). GIS-based frequency ratio and index of entropy models for landslide susceptibility assessment in the Caspian forest, northern Iran. International Journal of Environment Science and Technology. 11, 909–926.

[10] Lan, H. X., Zhou, C. H., Wang, L. J., Zhang, H. Y. & Li, R. H. (2004). Landslide hazard spatial analysis and prediction using GIS in the Xiaojiang watershed, Yunnan, China. Engineering Geology, 76, 109–128.

[11] Lee, S. & Choi, J. (2004). Landslide susceptibility mapping using GIS and the weight-of-evidence model. International Journal of Geographical Information Science. 18(8), 789–814.

[12] Lee, S. & Talib, J. A.(2005). Probabilistic landslide susceptibility and factor effect analysis. Environmental Geology. 47, 982–990.

[13] Meten, M., PrakashBhandary, N. & Yatabe, R. (2015). Effect of Landslide Factor Combinations on the Prediction Accuracy of Landslide Susceptibility Maps in the Blue Nile Gorge of Central Ethiopia. Geoenvironmental Disasters. 2(9), 1–17.

[14] Nettleton, I. M., Martin, S., Hencher, S. & Moore, R. (2005). Debris flow types and mechanisms. In M. G. Winter, F.

Macgregor, & L. Shackman, Scottish road network landslides study (pp. 45-67). Edinburgh: The Scottish Executive.

[15] Onda, Y. (1993). Underlying rock type controls of hydrological processes and shallow landslide occurrence. Sediment problems: Strategies for monitoring, prediction and control (pp. 47-55). Japan: IAHS Publication.

[16] Rasyid, A. A., Bhandary, N. P. & Yatabe, R. (2016). Performance of frequency ratio and logistic regression model in creating GIS based landslides susceptibility map at Lompobattang Mountain, Indonesia. Geoenvironmental Disasters. 3(19), 1–16.

[17] Reneau, S. L. & Dietrich, W. E. (1987). The importance of hollows in debris flow studies; Examples from Marin County, California. In J. E. Costa, & G. F. Wieczorek (Eds.), Debris Flows/Avalanches: Process, Recognition, and Mitigation. Virginia: Geological Society of America.

[18] Saadatkhah, N., Azman, K., Lee, M. L. & Gambo, H. (2015). Quantitative hazard analysis for landslides in Hulu Kelang area, Malaysia. Jurnal Teknologi. 73(1), 111–121.

[19] Sujatha, E. R. & Sridhar, V. (2017). Mapping Debris Flow Susceptibility using Analytical Network Process in Kodaikkanal Hills, Tamil Nadu (India). Journal of Earth System Science. 126(116), 1–18.

[20] Tangestani, M. H. (2004). Landslide susceptibility mapping using the fuzzy gamma approach in a GIS, Kakan catchment area, southwest Iran. Australian Journal of Earth Sciences. 51, 439-450.

[21] Xiaoqing, C., Peng, C., Yong, Y., Jiangang, C. & Deji, L. (2015). Engineering measures for debris flow hazard mitigation in the Wenchuan earthquake area. Engineering Geology. 194, 73–85.

[22] Yalcin, A., Reis, S., Aydinoglu, A. C. & Yomralioglu, T. (2011). A GIS-based comparative study of frequency ratio, analytical hierarchy process, bivariate statistics and logistics regression methods for landslide susceptibility mapping in Trabzon, NE Turkey. Catena. 85, 274–287.